

PCCP

Accepted Manuscript



This is an *Accepted Manuscript*, which has been through the Royal Society of Chemistry peer review process and has been accepted for publication.

Accepted Manuscripts are published online shortly after acceptance, before technical editing, formatting and proof reading. Using this free service, authors can make their results available to the community, in citable form, before we publish the edited article. We will replace this *Accepted Manuscript* with the edited and formatted *Advance Article* as soon as it is available.

You can find more information about *Accepted Manuscripts* in the [Information for Authors](#).

Please note that technical editing may introduce minor changes to the text and/or graphics, which may alter content. The journal's standard [Terms & Conditions](#) and the [Ethical guidelines](#) still apply. In no event shall the Royal Society of Chemistry be held responsible for any errors or omissions in this *Accepted Manuscript* or any consequences arising from the use of any information it contains.

Silver nanoparticle aided self-healing of polyelectrolyte multilayers

Cite this: DOI: 10.1039/x0xx00000x

Xiayun Huang,^a Matthew J. Bolen,^b and Nicole S. Zacharia^{*a,c}

Received 00th January 2012,
Accepted 00th January 2012

DOI: 10.1039/x0xx00000x

www.rsc.org/

Self-healing is the ability of a material to repair mechanical damage. The lifetime of a coating or film might be lengthened with this capacity. Water enabled self-healing of polyelectrolyte multilayers has been reported, using systems that grow via the interdiffusion of polyelectrolyte chains. Due to high mobility of the polyelectrolyte chains within the assembly, it is possible for lateral diffusion to heal over scratches. The influence of metal ions and nanoparticles on this property has, however, not been previously studied. Here we demonstrate that the incorporation of silver nanoparticles reduced *in situ* within in the branched polyethylene imine/polyacrylic acid polyelectrolyte multilayer structure speeds the ability of the multilayer assembly to self-heal. This enhancement of property seems to not be due to changes in mechanical properties but rather in enhanced affinity to water and plasticization that enables the film to better swell.

1. Introduction

The layer-by-layer (LbL) method for directing the complexation of oppositely charged polyelectrolytes has proven to be a powerful and versatile tool for creating thin films and coatings (called polyelectrolyte multilayers or PEMs) composed of a range of components including but not limited to polymers (such as nanoparticles, oligomers, surfactants, and various biomaterials).¹⁻⁵ These coatings have been proposed in use for a range of applications, but one of the remaining challenges for these materials when considering moving them from the laboratory to the real world is mechanical robustness.³ This includes not only strength as represented by a high Young's modulus, but other factors as well such as toughness, cracking, adhesion to the underlying substrate, and resistance to wear.^{3,6-9} Most LbL films are made from commercially available polyelectrolytes, which limits the range of possible mechanical properties. A related property that deals with materials' use and lifespan is the ability to self-heal, or to somehow mitigate physical damage.¹⁰

A common way to improve the mechanical properties of polymer thin films is the inclusion of metal or other inorganic nanoparticles.⁵ Due to their small size, metal nanoparticles often have properties that are different from those of bulk metals. These novel properties may find application in areas such as photoelectronics, catalysis, magnetism, and sensing in addition to their mechanical benefits.⁵ As well as metal nanoparticle containing films showing increased mechanical behavior, PEMs containing metal ions have been shown to possess improved mechanical properties.¹¹ The addition of Cu²⁺

to BPEI/PAA PEMs has been shown to increase both the modulus and hardness and these changes in mechanical properties can be tuned with Cu²⁺ concentration, which in turn can be controlled by the specific assembly procedure.¹¹

The work presented here looks at the self-healing ability of PEMs containing metal nanoparticles and ions. A range of self-healing strategies has been demonstrated for polymeric and supramolecular materials including encapsulated healing agent (generally monomer) that bursts open upon mechanical damage or the use of various reversible bonding schemes, covalent and non-covalent.^{10,12-16} In the case of incorporating healing agent there are some difficulties regarding the embedding of the agent (which sometimes must include catalyst) and keeping it from reacting before physical damage occurs, and then providing for sustained release once the damage does happen.¹⁰ On the other hand reversible bonding schemes generally have some limitations and often need an external stimulus to operate such as light or heat.^{12,13}

To date, there are several literature reports of self-healing within PEM systems.¹⁷ The general strategy for self-healing with LbL films tends to be to make use of chain diffusion within the multilayer assembly or the mobility of small molecules or other healing agents that are co-deposited along with the polyelectrolytes. Quite often the presence of water or high amounts of humidity is required for self-healing to occur. These reports of self-healing PEMs usually rely on the so-called exponentially growing PEM systems wherein the polymer chains are very mobile and some degree of unbound polyelectrolyte chains remain in the film.¹⁸ In these systems the unbound material is able to laterally diffuse to the site of a scratch or other kind of damage and heal the film. Specifically, the branched

polyethylene imine (BPEI)/ polyacrylic acid (PAA) PEM system has been reported by Sun, *et al.*, to have self-healing properties when submerged in water.¹⁸ Shchukin *et al* report anti-corrosion coatings incorporating BPEI with other polyelectrolytes (PAA as well as sulfonated polystyrene) and found that one of the beneficial aspects of PEMs for anti-corrosion coatings is their ability to laterally diffuse and heal over cracks that might come to be formed in the coating.¹⁹ In another example, both superhydrophobicity and self-healing were combined, showing that the LbL technique is a good method for combining functionalities within one thin film.²⁰

Here, we report on the influence of the addition of silver ions and particles of various sizes to the self-healing ability of BPEI/PAA. Thanks to the branched structure of BPEI, which contains primary, secondary and tertiary amino groups in a ratio of 1:2:1,²¹ the polymer has the ability to form a complex with Ag^+ (or other metal) ions.¹¹ Water allows the PEMs to soften and flow, and we demonstrate that the formation of silver nanoparticles somehow enhances this effect, possibly through a plasticization of the PEM.

2. Experimental

2.1. Materials

Branched poly(ethyleneimine) (BPEI, $M_w=25,000$) was obtained from Sigma-Aldrich and poly(acrylic acid) (PAA, $M_w=50,000$, 25 wt% solution) was purchased from Polysciences Inc. Sodium borohydride (NaBH_4) and silver nitrate (AgNO_3) were purchased from EMD and formaldehyde (35 wt%) were from Alfa Aesar. 4-(2-hydroxyethyl)-1-piperazineethanesulfonic acid (HEPES) was purchased from Amresco. De-ionized (DI) water with 18.2 $M\Omega\cdot\text{cm}$ resistivity from a Milli-Q filtration system was used for all experiments. All materials were used as received without further purification.

2.2. Characterization

Film thickness was measured using a stylus profilometer (KLA Tencor Instruments P6), and values reported represent an average of 5 different position of the film. Static water contact angle values were measured using a VCA Optima system (AST products Inc.) equipped with a video camera at room temperature with DI water (18.2 $M\Omega\cdot\text{cm}$) as a probe fluid (1.5 μL). PEM were stored in an environment with relative humidity of ~55% for over 24 h before the test. Each contact angle reported was the average value of 5 independent measurements in each case. An optical microscope (VHX-600, Keyence Co.) was used for *in-situ* observation of the films' self-healing properties with a long working distance and wide depth of field lens (VH-Z100). The 30 bilayer thick films grown on glass slides were cut into 1 $\text{cm}\times 2.5$ cm pieces and then scratched with a razor blade. The film was then submerged into 10 mL of DI water. The *in-situ* observation started from the time of immersion. Time lapse images of the films underneath water were also taken every 10 min till the film healed or continued for as long as 60 min if healing was not complete. After the healing test the films were allowed to dry in the same 55% relative humidity atmosphere in which they had originally been stored for 5 hours and then photographed again. Transmission electron microscopy (TEM) images were taken using a FEI Tecnai G2 F20 microscope operated at 200 kV and the JEOL 1200 EX microscope operated at 100 kV. The free-standing

films were dissolved in 1 mmol/L HNO_3 solution and cast drop onto 200 mesh carbon film supported copper grids (TED PELLA, Inc). After having completely dried, the specimens were stored in a desiccator for a few hours before observation and the TEM images were always taken within a few hours. FTIR spectra were obtained using an IR Prestige 21 system (Shimadzu Corp., Japan) and analyzed by IRsolution V.1.40 software. Films coated on silicon wafer were measured via attenuated total reflection (ATR) mode. UV-vis measurements were performed on a UV-2250 system (Shimadzu Corp., Japan). To study the water uptake of the various films, each film was assembled on a glass slide and immersed in 140 mL of DI water for various times. Mass uptake was measured using an Excellence XS analytical balance (Mettler Toledo, Switzerland). The film was then immersed into 1 mol/L HCl for 30 min in order to decompose the film. The mass of water uptake of each of the polyelectrolyte films were calculated by subtracting out the mass of glass slide. The surface Young's modulus of the film was measured by Atomic Force Microscopy (Bruker Dimension Icon AFM, Germany) through Peak Force Quantitative Nanomechanical Property Mapping mode using silicone probe with a spring constant of 5 N/m. The modulus was obtained by fitting the force-displacement curve with the Hertzian model using data that was collected from ~10 different positions. All measurements were done at room temperature with the relative humidity of ~30%.

2.3. Polyelectrolyte Multilayer (PEM) Assembly

PEMs were assembled on glass slides, silicon wafers, and polystyrene substrates. Before use, the glass slides and silicon wafers were treated in a freshly prepared piranha solution (mixture of H_2SO_4 (98%) and H_2O_2 (30%) with a volume ratio of $v/v=7/3$) at room temperature for 4 h and then rinsed with DI water until neutralized. The polystyrene substrates were rinsed with ethanol and then DI water. All the substrates were dried by nitrogen steam before being used for layer-by-layer assembly.

BPEI/PAA multilayer films were assembled using concentrations of 80 mmol/L BPEI and 60 mmol/L PAA with respect to the functional group (either amine groups or carboxylic acid groups). The pH of these solutions was adjusted with 1 mol/L NaOH or 1 mol/L HNO_3 solution to pH 9.5 for the BPEI solution and pH 4.5 for the PAA solution. All multilayer assembly was carried out at room temperature using a StratoSequence VI dipper (NanoStrata Inc.). The cleaned and dried substrates were first exposed to BPEI solution for 10 min followed by three separate DI water rinse baths. Then, the substrates are exposed to PAA solution for 10 min again followed by three DI water rinse baths. This cycle was repeated until desired bilayers were reached. The multilayer films were dried at room temperature (~25°C and relative humidity at ~55%) for 24 h before any testing.

BPEI- Ag^+ /PAA multilayer films were prepared using a stable complex of the polycation BPEI (concentration 80 mmol/L with respect to the functional group) and silver nitrate (concentration 1 mmol/L) and the negative polyanion PAA (60 mmol/L with respect to the repeating unit). The assembly pH and procedure were the same as for the BPEI/PAA multilayer films.

BPEI- Ag NP/PAA multilayer films were fabricated by reducing the Ag^+ ions in the BPEI- Ag^+ /PAA multilayer film using a 10 mmol/L NaBH_4 solution. BPEI- Ag^+ /PAA multilayer films were immersed in NaBH_4 solutions for 30 min then followed by 1 min of water rinsing. The wet film was dried for 24 h before any tests.

BPEI-Ag NC/PAA multilayer films were then prepared using a silver nanocluster (Ag NC) dispersion in BPEI solution (80 mmol/L with respect to the functional group) with the same concentration of negative polyanion PAA. The Ag NC was synthesized following the literature.¹⁹ Silver ions were sequestered in the branched PEI and reduced by formaldehyde. BPEI (0.094 g/mL, 100 μ L) and HEPES (1 mmol/L, 50 μ L) were first dissolved in DI water (95 μ L) by stirring for 2 min. Then, AgNO₃ (100 mmol/L, 250 μ L) was added and homogenized by stirring for another 2 min. Finally, formaldehyde (5 μ L) was added under vigorous stirring. The resultant solution was heated at 70°C for 10 min, cooled at room temperature, and stored at 4°C for over 48 h before use. The assembly pH and procedure were the same as BPEI-Ag NC/PAA and BPEI/PAA multilayer films.

3. Results and discussions

Polyelectrolyte multilayer films of BPEI and PAA as well as those containing Ag⁺ ions, Ag nanoparticles (Ag NP), or Ag nanoclusters (Ag NC)²² were fabricated using typical layer-by-layer deposition procedures. Fig.1 shows the film thickness versus the number of deposition bilayers as well as images of the films showing different colors formed by the incorporation of different types of silver. The film thicknesses increase exponentially during the first 15 bilayers, following the “in and out” diffusion mechanism.²³ For films of this type one (or both) of the polyelectrolytes are able to not only to add on to the surface of the LbL film but to diffuse into the bulk of the film. Then during subsequent deposition steps this ‘extra’ polymer diffuses back out and complexes with material at the film’s surface. In a manner consistent with the reported growth of BPEI/PAA PEMs,^{18,29} the thickness values then switch to a linear growth regime forming films as thick as ~25 μ m within 25 or 30 bilayers.

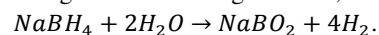
Thanks to its branched structure and the ratio of primary, secondary, and tertiary amine groups present,^{21,24} BPEI can form a stable complex with most of the transition metal ions, such as Ag⁺ and Cu²⁺,¹¹ over a wide range of ion concentrations. These stable complexes can then be used in polyelectrolyte assembly with negatively charged PAA.¹¹ The growth of BPEI-ion complex/PAA follows the trend of BPEI/PAA with exponential growth during the first 15 bilayers³⁰ and a very thickly depositing linear growth thereafter. The thickness of BPEI-Ag⁺/PAA is slightly less than that of BPEI/PAA above 20 bilayers due to the increased crosslink density introduced by the silver ions and their interactions with both carboxylic acids and amine groups. An enlargement of the growth curve can be seen in figure S1 in order that the non-linear part of the growth curve can be seen more clearly.

Although the concentration of Ag⁺ in the BPEI assembly solution is as low as 1 mmol/L, silver ion is incorporated into the BPEI-Ag⁺/PAA films, which are transparent (fig. 1). When the BPEI-Ag⁺/PAA film was exposed to a reducing environment to form silver particles *in situ* by using a 10 mmol/L NaBH₄ aqueous solution, the transparent film will change to dark brown gradually over the course of 30 minutes due to the formation of Ag nanoparticles from the Ag⁺ already

embedded in the film.^{22,25} The size of the Ag nanoparticles formed in the PEM though *in situ* reduction are 54.8 nm \pm 21 based on measuring the size of 300 particles, shown in supporting information Fig. S2. The creation of these Ag nanoparticles does not make any appreciable changes in film thickness. The reduction of silver ions can be confirmed visually with the evolution of an orange-brown color which is the surface plasmon resonance of the silver nanoparticles. Figure S7 shows the UV-vis spectrum of a BPEI-Ag⁺/PAA film on quartz, which has no significant features in the UV-vis and the spectrum of that film once reduced. Two features can be seen, one at about 275 nm and one at about 360 nm.

In order to test the influence of particle size, in addition to the BPEI/PAA films with *in situ* reduced particles, another kind of particle containing PEM was fabricated. Ag nanoclusters approximately 5 nm in size (average of 5.5 nm \pm 1.3 based on 300 particles, shown in supporting information Fig. S2) and BPEI were mixed together and used as the positively charged polyelectrolyte for the multilayer assembly. The branched structure of BPEI allows for silver particles (5.4 mg/mL) to be partitioned into its structure,²¹ forming a stable solution for weeks. Film assembly using the particle dispersion follows the same growth trend observed in the previously discussed cases and a film 20 μ m in thickness is formed with 30 bilayers. Due to the small size of the silver clusters, the color of the Ag NC containing film was much lighter than the PEM with the *in situ* reduced particles.

From FTIR spectroscopy of all the films in wet and dry state (figure S3), we can see that the introduction of silver in any of these forms does not change the degree of ionization within the PEM films. Furthermore, we can see that from the FTIR of a BPEI/PAA film before and after exposure to NaBH₄ solution (figure S4) that there are no chemical changes to the polymers within the multilayers. NaBH₄ will react with water to form sodium metaborate, and relatively quickly at neutral and acidic pH values according to the following reaction;²⁶



The metaborate anion may exist as dimers or other associations or hydrates in solution. It is possible that the film is swelled with the sodium metaborate, although we do not see the FTIR peaks associated with borate. It is possible that some of these signals are lost in either water peaks, as sodium metaborate has a strong peak at about 3400 wavenumbers, and peaks at 1655 and 1310 wavenumbers which could be obscured by the PEM itself, especially if the amounts are small.²⁷

However, for the BPEI-Ag NP/PAA films soaking in water continuously over the course of 48 hours does seem to create some rearrangement in the film, forming pores (figure S5). Chain exchange with the surrounding environment in known to happen in some polyelectrolyte multilayer systems, especially in those that are exponentially growing.^{28,29} By soaking the BPEI-Ag NP/PAA film in water for 48 hours, taking the solution in which the film was soaked, drying it and taking FTIR of the residue (figure S6) it does seem that there is a small amount of polyelectrolyte that is dissolved from the film into the solution over the 48 hours.

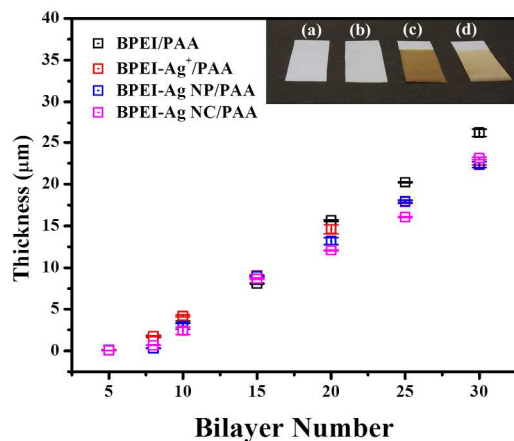


Fig. 1 The growth curves of polyelectrolyte multilayer films. (a) BPEI/PAA, (b) BPEI-Ag⁺/PAA, (c) BPEI-Ag NP/PAA and (d) BPEI-Ag NC/PAA. All PEMs follow the exponential growth initially and rapid linear growth afterwards. Insert pictures show the 30 bilayer PEMs deposited on the white polystyrene films.

The self-healing ability of the four different types of 30 bilayer films immersed in water was tested. Scratches were made by razor blade on dried films, completely scratching through the film to the substrate. For the samples depicted in fig. 2, the scratch widths are 89 μm for the BPEI/PAA film, 135 μm for the BPEI-Ag⁺/PAA film, 60 μm for the BPEI-Ag NC/PAA film, and 76 μm for the BPEI-Ag NP/PAA film. Differences in scratch size are due to them being made manually. Fig. 2 shows images of the scratch under water as time passes. The scratch on a BPEI-Ag NP/PAA film can be healed within 10 min (corresponding healing movies are shown in supporting information, Movie S1), while none of the other films can be healed after even 60 min water immersion. However, in the cases when complete healing is not achieved the size of the scratch is slightly reduced over the course of 60 minutes. Fig. 3 shows a set of scratched films before immersion in water (a1, b1, c1, d1) and after immersion for 10 minutes and then immediately being dried to capture the morphology present at that time (a2, b2, c2, d2). The scratches on these samples were made in the same way as for the samples in fig. 2. One can again see that the BPEI-Ag NP/PAA film was re-healed much faster than the other films. The scratch on the BPEI/PAA film is also noticeably smaller after 10 min of water immersion, but the same cannot be said for the other films. Elsewhere in the literature BPEI/PAA without any additives has been reported to have better self-healing properties than we report here,¹⁸ but these films were assembled with different pH conditions and using a higher molecular weight of BPEI. We believe that the assembly conditions are the dominant factor in determining self-healing as this dictates the amount of 'excess' polyelectrolyte present within the film, but the rheological properties of the system may also be influenced by molecular weight.

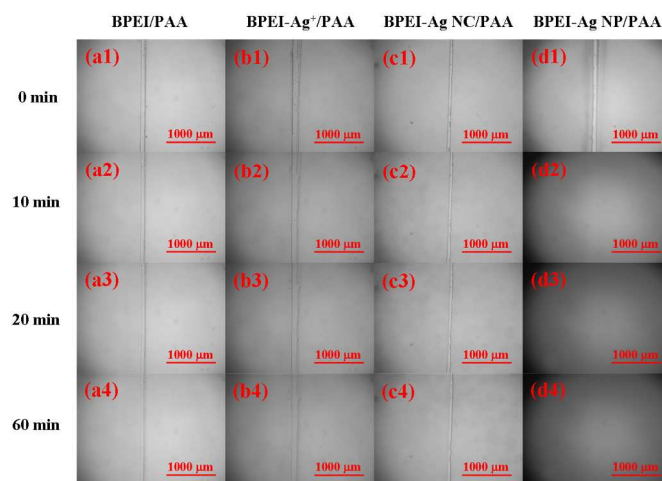


Fig. 2 Time lapse optical micrographs of scratched films immersed in water for as long as 60 min. (a1-a4) 30 bilayers film of BPEI/PAA with a 89 μm scratch (b1-b4) BPEI-Ag⁺/PAA film, scratch width 135 μm (c1-c4) BPEI-Ag NC/PAA film, scratch width 60 μm, and (d1-d4) BPEI-Ag NP/PAA film with a 76 μm wide scratch underneath water for 0 min, 10 min, 20 min and 60 min, respectively. The BPEI-Ag NP/PAA film can be completely healed after 10 min, however other films cannot be healed even till 60 min immersed in the water.

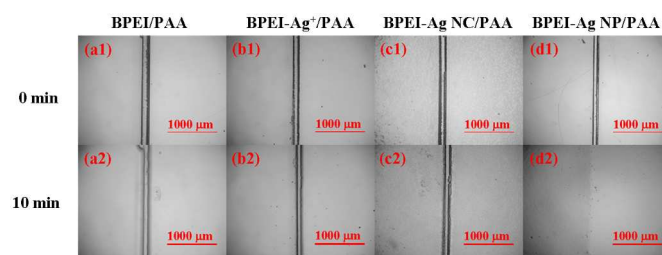


Fig. 3 Optical microscope images of self-healed properties of dried film before water immersion and after water immersion for 10 min. (a1-a2) 30 bilayers of dried BPEI/PAA film (b1-b2) BPEI-Ag⁺/PAA film, (c1-c2) BPEI-Ag NC/PAA film, and (d1-d2) BPEI-Ag NP/PAA and dried film after 10 min water immersion, respectively.

The self-healing ability of several other cases was examined in order to glean further insights into the mechanism of this self-healing. As previously discussed, a small amount of polyelectrolyte seems to dissolve over the course of 48 hours, but this does not seem to be an important factor over the course of 10 minutes or so. The self-healing ability of BPEI/PAA films not containing any silver and exposed to NaBH₄ solution for 1 min and 30 minutes was also examined. For 1 min of NaBH₄ exposure no difference in healing is noticed as compared to the as assembled film. For the case of 30 minutes of NaBH₄ exposure the healing process is faster than for a BPEI/PAA film as assembled, but still not as fast as the film with Ag NPs. Swelling in NaCl solution for any amount of time does not impact the swelling ability. As discussed above, the NaBH₄ solution will actually contain associations and hydrates of BO₂⁻ ion, which we hypothesize will swell the multilayer in a manner that other salts (e.g. NaCl) will not, perhaps because of the size of those anion dimers. Although we do not see changes in the film's FIR spectrum, indicating that at the very least if there is swelling by borate it is not a significant amount that infiltrates

the film, there does seem to be some contribution from the salt in our observed self-healing.

Films containing contrasting amounts of silver nanoparticles were also examined. Films were assembled with 3 mmol and 6 mmol of Ag^+ in the BPEI solution. These films with increased silver loading are darker and much more rough (figure S9), in agreement with literature reports.³⁰ These films both are able to heal in a shorter time than the film made with 1 mmol of Ag^+ ion (seen in figure S10), with the cut seemingly healed in approximately 5 minutes, but there is no appreciable difference between the healing of the two films. The addition of Ag^+ ion in the film will increase both the size as well as the density of NPs created during *in situ* reduction.^{25,31} Therefore it is difficult to say which is the more important parameter regarding the NPs, their size or quantity.

This self-healing property under water seems to be related to the ability the PEM network to flow and swell. The addition of larger nanoparticles seems to change these properties while addition of very small particles and ions only does not make any changes in self-healing. One possible explanation is possibly the affinity to water of these different materials. That is, perhaps systems that take up more water more quickly are also able to self-heal more quickly. For this reason, the relative hydrophobicity of these different systems was investigated.

The water contact angle of the BPEI/PAA PEM (Fig. 4) without Ag ion or Ag particles is $\sim 75^\circ$, which is higher than either reports of multilayer film contact angles with either BPEI or PAA as the outermost layer³²⁻³⁴ and also is higher than measured contact angles for monolayers and implies that the film surface is composed of more C-H polymer backbone than amine or carboxyl groups as compared to the monolayer case. This could be because the motion of these charged groups is hindered when they form the complex. The partition of polymer backbone to the surface results in a slightly higher water contact angle. However, the addition of silver decreases the contact angle sharply to about $\sim 45^\circ$. The presence of Ag^+ ion near the film surface increases affinity to water and the same low contact angle value is observed for PEMs with Ag nanoparticles and clusters, as shown in fig. 4.

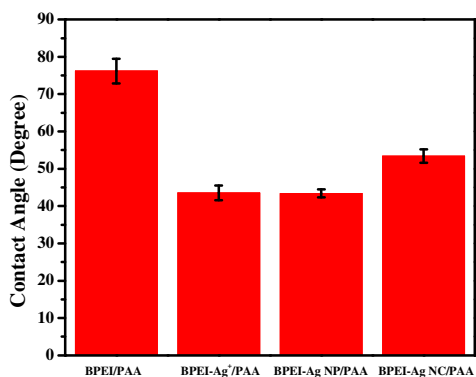


Fig. 4 Static water contact angle of polyelectrolyte multilayer films. (a) BPEI/PAA, (b) BPEI-Ag⁺/PAA, (c) BPEI-Ag NP/PAA and (d) BPEI-Ag NC/PAA. Water contact angle decreases from $\sim 75^\circ$ to $\sim 45^\circ$ from the introduction of Ag^+ ion or Ag particles to the PEMs.

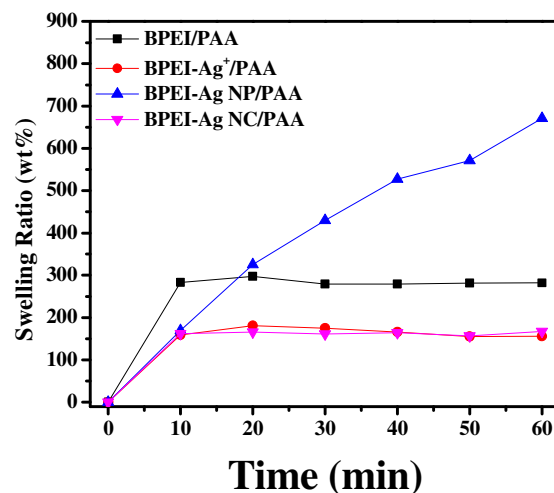


Fig. 5 The swelling ratio of 30 bilayers polyelectrolyte multilayer films immersed in the water for different time periods. The water uptake behaviors of BPEI-Ag⁺/PAA and BPEI-Ag NC/PAA were similar. However, these behaviors of BPEI/PAA and BPEI-Ag NP/PAA were quite different.

Water uptake for these systems was also measured. The results of this measurement follow a now familiar trend. All of these films do swell once immersed in the water, but they have quite different swelling ratios. Here the swelling ratio is defined as the fractional increase in the weight of the film due to water absorption. As shown in fig. 5, both BPEI-Ag⁺/PAA and BPEI-Ag NC/PAA films swell ~ 150 wt%. The swelling happens in the first 10 min and the water uptake reaches a plateau after this time. In comparison, the swelling ratio for BPEI/PAA film is $\sim 300\%$ which is nearly twice that of both BPEI-Ag⁺/PAA and BPEI-Ag NC/PAA films. This process is also saturated very quickly, during the first 10 min of exposure to water. Interestingly, the BPEI-Ag NP/PAA film took up water continuously to almost $\sim 700\%$, a process that did not saturate within 60 min of water immersion. As can be seen in figure S8 this water uptake continues for some 10 or so hours when it begins to decrease again, corresponding with the formation of porous features in the film. This large difference in water uptake behavior may point to the reason why the BPEI-Ag NP/PAA film was able to heal in the presence of water much faster than all other films. The BPEI/PAA film also swells much more than BPEI-Ag⁺/PAA and BPEI-Ag NC/PAA films and has the second greatest ability to self-heal after 10 min of water immersion shown in fig. 3 (a2). We hypothesize that the properties of the NP containing film is due to plasticization from both the metaborate ions and the nanoparticles themselves.

The elastic modulus of this series of films was measured using AFM. The results can be seen in fig. 6. Although Cu^{2+} ions have been shown to increase PEM modulus,¹¹ in the case

of the addition of silver the modulus of BPEI/PAA, BPEI-Ag⁺/PAA, and BPEI-Ag NP/PAA were all approximately the same (close to 3 GPa) within the error of the measurement. Interestingly, the BPEI-Ag NC/PAA film is somewhat softer at a little over 1 GPa. Multivalent ions have been shown to enhance mechanical properties because of their ability to act as crosslinkers. The monovalent silver does not act in this capacity. One possible explanation is that the each silver ion is binding with only one functional group, and therefore not crosslinking the film.

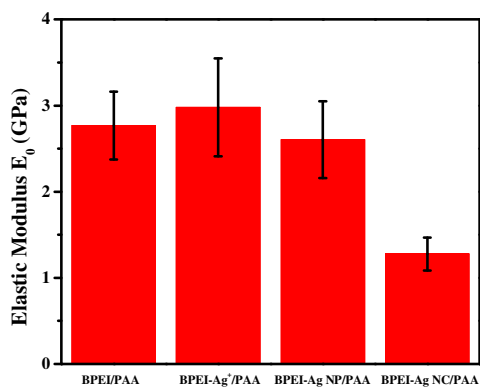


Fig. 6 Surface Young's modulus E_0 determined by the AFM nanoindentation technique for 30 bilayers polyelectrolyte multilayer thin film (a) BPEI/PAA, (b) BPEI-Ag⁺/PAA, (c) BPEI-Ag NP/PAA and (d) BPEI-Ag NC/PAA. The thicknesses of these films were ~ 25 μm .

Although scratch healing was chosen as the demonstration of self-healing properties of the polyelectrolyte thin film, this demonstration also depends on factors such as the thickness of the film, the width of scratches, and adhesion to the substrate. Adhesion to the substrate might in particular slow the lateral diffusion of polyelectrolyte chains, especially in very thin films. Inspired by demonstrations of self-healing hydrogels, four types of free-standing polyelectrolyte thin films were made with the same assembly procedure as previously and deposited on a polystyrene substrate instead of glass slide or silicon wafer. The films were cut into 1 cm \times 1 cm pieces before being fully dried. In this way, once fully dried they can be easily peeled off from the polystyrene substrate due to the weak hydrophobic interactions between the film and the substrate. Due to the hydrophilicity of all of these films, they become tacky and hydrogel-like once they are rehydrated with water (here using a spray bottle). As in the case of healable hydrogels,³⁵ water acts as a plasticizer within the polyelectrolyte multilayers, allowing for the interdiffusion of BPEI and PAA chains at the various film interfaces. Moreover, using water of neutral pH ensures some extent of degree of ionization of both amino and carboxyl groups of the BPEI and PAA and the formation of new ionic bonds, ensuring a strong interface. Weakness at healed interfaces is often an issue in self-healed materials, and the

ability to locally reform bonds may be an advantage of PEM systems.

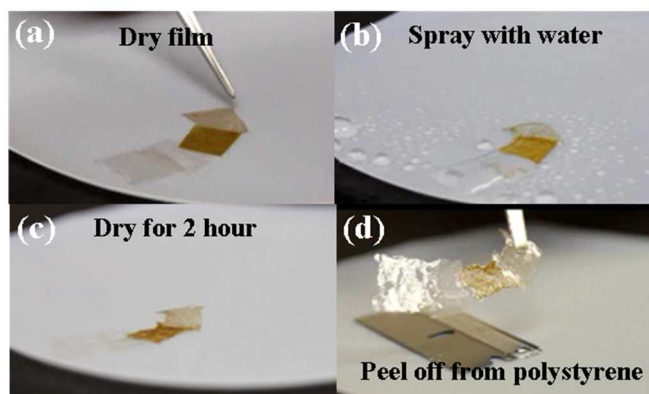


Fig. 7 Illustration of self-healing properties of free standing polyelectrolyte film segments. (a) Dried films of BPEI/PAA, BPEI-Ag⁺/PAA, BPEI-Ag NP/PAA and BPEI-Ag NC/PAA (from left to right) were placed on a polystyrene surface slightly overlapping. (b) The dried films were then sprayed with water. (c) The films become tacky and are able to reconfigure into one piece over the course of 2h while the water evaporates. (d) The resultant "healed" film which contains all of the original PEM segments is peeled off from the polystyrene substrate. The corresponding movie of this self-healing property is shown in supporting information Movie S2.

4. Conclusions

We have demonstrated that polyelectrolyte multilayer systems made from BPEI/PAA have enhanced ability to self-heal in water with the addition of silver nanoparticles reduced *in situ* within the film. This self-healing is a matter of the film being able to swell sufficiently for polyelectrolyte chains to move across the damage area and reform ionic interactions. Addition of silver ions alone or silver nanoclusters does not give this enhancement in property. The process of soaking the film in the NaBH₄ solution also participates in enhancing the self-healing ability, although increasing silver content also increases self-healing to a certain extent. We have also found that the assembly conditions, that is the pH of the polyelectrolyte assembly solutions, seems to create differences in self-healing ability when comparing our work to literature reports. These differences in the pH create different charge densities along the polyelectrolyte backbones which then lead to different amounts of polymer diffusing in and out of the film. A film with more "reservoir" of polyelectrolyte or just more chain mobility will then have a greater ability to heal over a scratch.

The enhanced healing ability of the nanoparticle containing film does not seem to have to do with changes in mechanical properties as those films have about the same modulus as the multilayers with no additional silver. Neither are the charge densities of the various polyelectrolytes changing during the formation of the nanoparticles within the film. Instead, it seems that hydrophilicity and water uptake are more important factors in the film's ability to self-repair. We hypothesize that plasticization of the PEM is taking place, increasing ability to swell. These findings should enable us to better design next generation polyelectrolyte based self-healing materials.

Acknowledgements

The authors thank the American Association of Railroads as well as student support through NSF under award DMR-1255612. The

authors also thank Dr Karen L. Wooley for use of her FTIR instrument and photographer, Sin Dik (Cindy) Ma, helps with taking videos and photos, as well Dr. Wilson Serem for help with the AFM measurements of film modulus.

Notes and references

^aTexas A&M University, Department of Mechanical Engineering, College Station, TX, 77843, USA.

^bTexas A&M University, Department of Chemical Engineering, College Station, TX, 77843, USA

^cThe University of Akron, Department of Polymer Engineering, Akron, OH, 44325, USA.

*To whom correspondence should be addressed.

E-mail: [n zacharia@uakron.edu](mailto:nzacharia@uakron.edu); Fax: 1 330 972 3406; Tel: 1 330 972 8248

† Electronic Supplementary Information (ESI) available: [TEM image of Ag nanoparticles and Ag nanoclusters, FTIR spectra of dried and wet film, UV-vis of the reduction of silver within the film, Self-healing property of in-situ optical microscope movie of BPEI-Ag NP/PAA film, Self-healing demo movies of BPEI/PAA, BPEI-Ag⁺/PAA, BPEI-Ag NP/PAA and BPEI-Ag NC/PAA film with each other with water spray]. See DOI: 10.1039/b000000x/

- 1 P. T. Hammond, *Adv. Mater.*, 2004, **16**, 1271-1293.
- 2 P. Lavalle, J. C. Voegel, D. Vautier, B. Senger, P. Schaaf and V. Ball, *Adv. Mater.*, 2011, **23**, 1191-1221.
- 3 Y. Li, X. Wang and J. Sun, *Chem. Soc. Rev.*, 2012, **41**, 5998-6009.
- 4 M. S. Johal and P. A. Chiarelli, *Soft Matter*, 2007, **3**, 34-46.
- 5 S. Srivastava and N. A. Kotov, *Accounts of Chemical Research*, 2008, **41**, 1831-1841.
- 6 Z. Tang, N. A. Kotov, S. Magonov and B. Ozturk, *Nat. Mater.*, 2003, **2**, 413-418.
- 7 P. Podsiadlo, A. K. Kaushik, E. M. Arruda, A. M. Waas, B. S. Shim, J. Xu, H. Nandivada, B. G. Pumplun, J. Lahann, A. Ramamoorthy and N. A. Kotov, *Science*, 2007, **318**, 80-83.
- 8 P. Podsiadlo, M. Michel, J. Lee, E. Verploegen, N. W. S. Kam, V. Ball, J. Lee, Y. Qi, A. J. Hart, P. T. Hammond and N. A. Kotov, *Nano Lett.*, 2008, **8**, 1762-1770.
- 9 X. Liu, L. Zhou, F. Liu, M. Ji, W. Tang, M. Pang and J. Sun, *J. Mater. Chem.*, 2010, **20**, 7721-7727.
- 10 B. J. Blaiszik, S. L. B. Kramer, S. C. Olugebefola, J. S. Moore, N. R. Sottos and S. R. White, *Annu. Rev. Mater. Res.*, 2010, **40**, 179-211.
- 11 X. Huang, A. B. Schubert, J. D. Chrisman and N. S. Zacharia, *Langmuir*, 2013, **29**, 12959-12968.
- 12 S.D. Bergman and F. Wudl, *J. Mater. Chem.* 2008, **18**, 41 – 62.
- 13 Cordier, P.; Tournilhac, F.; Soulié-Ziakovic, C.; Leibler, L. *Nature* 2008, **451**, 977-980.
- 14 D. G. Shchukin, *Polym. Chem.*, 2013, **4**, 4871-4877.
- 15 D. G. Shchukin and H. Mohwald, *Small*, 2007, **3**, 926-943.
- 16 L.R. Hart, J.L. Harries, B.W. Greenland, H.M. Colquhoun, W. Hayes, *Polym. Chem.* 2013, **4**, 4860 – 4870.
- 17 E.V. Skorb and D.V. Andreeva, *Polym. Chem.*, 2013, **4**, 4834 – 4845.
- 18 X. Wang, F. Liu, X. X. Zheng and J. Sun, *Angew. Chem. Int. Ed.*, 2011, **50**, 11378-11381.
- 19 D. V. Andreeva, E. V. Skorb and D. G. Shchukin, *ACS Applied Materials & Interfaces*, 2010, **2**, 1954-1962
- 20 Y. Li, L. Li, J. Sun, *Angew. Chem., Int. Ed.*, **2010**, **49**, 6129.
- 21 K. Shiro, H. Kazuhisa, T. Masazumi and S. Takeo, *Macromolecules*, 1987, **20**, 1496-1500.
- 22 F. Qu, N. B. Li and H. Q. Luo, *J. Phys. Chem. C*, 2013, **117**, 3548-3555.
- 23 C. Picart, J. Mutterer, L. Richert, Y. Luo, G.D. Prestwich, P. Schaaf, J.-C. Voegel, P. Lavalle, *Proc. Natl. Acad. Sci. USA* 2002, **99**, 12531 – 12535.
- 24 J. Fu, J. Ji, L. Shen, A. Küller, A. Rosenhahn, J. Shen and M. Grunze, *Langmuir*, 2009, **25**, 672-675.
- 25 J. Dai and M. L. Bruening, *Nano Lett.*, 2002, **2**, 497-501.
- 26 H.I. Schlesinger, H.C. Brown, A.E. Finholt, J.R. Gilbraith, H.R. Hoekstra, and E. K. Hyde, *J. Am. Chem. Soc.*, 1953, **75**, 215 – 219.
- 27 F.A. Miller, C.H. Wilkins, *Anal. Chem.* 1952, **24**, 1253 – 1294.
- 28 H.W. Jomaa and J.B. Schlenoff, *Langmuir*, 2005, **21**, 8081-8084.
- 29 N.S. Zacharia, M. Modestino and P.T. Hammond, *Macromolecules*, 2007, **40**, 9523 – 9528.
- 30 J. Ji, J. Fu and J. Shen, *Adv. Mater.*, 2006, **18**, 1441-1444.
- 31 T.C. Wang, M.F. Rubner, R.E. Cohen, *Langmuir* 2002, **18**, 3370 – 3375.
- 32 Q. Tan, J. Ji, M. A. Barbosa, C. Fonseca and J. Shen, *Biomaterial*, 2003, **24**, 4699-4705.
- 33 B. Thierry, F. M. Winnik, Y. Merhi, J. Silver and M. Tabrizian, *Biomacromolecules*, 2003, **4**, 4564-4571.
- 34 S. G. Boyes, B. Akgun, W. J. Brittain and M. D. Foster, *Macromolecules*, 2003, **36**, 9539-9548.
- 35 A. Phadke, C. Zhang, B. Arman, C. C. Hsu, R. A. Mashelka, A. K. Lele, M. J. Tauber, G. Arya and S. Varghese. *PNAS*, 2012, **109**, 4383-4388.